

3

The Anatomical Foundation for Multidisciplinary Studies of Animal Limb Function: Examples from Dinosaur and Elephant Limb Imaging Studies

John R. Hutchinson¹, Charlotte Miller¹, Guido Fritsch², and Thomas Hildebrandt²

3.1 Introduction

What makes so many animals, living and extinct, so popular and distinct is anatomy; it is what leaps out at a viewer first whether they observe a museum's mounted *Tyrannosaurus* skeleton or an elephant placidly browsing on the savannah. Anatomy alone can make an animal fascinating – so many animals are so physically unlike human observers, yet what do these anatomical differences mean for the lives of animals?

The behavior of animals can be equally or more stunning- how fast could a *Tyrannosaurus* move (Coombs 1978; Alexander 1989; Paul 1998; Farlow et al. 2000; Hutchinson and Garcia 2002; Hutchinson 2004a,b), or how does an elephant manage to momentarily support itself on one leg while 'running' quickly (Gambaryan 1974; Alexander et al. 1979; Hutchinson et al. 2003, 2006)? Yet to attain a fundamental understanding of many animal behaviors we must venture beneath their skin surface and analyze the anatomical structures that constrain and enable visible behaviors. An elephant does not manage the aforementioned unipodal feat by sheer willpower or neurological activity alone – muscles, tendons, and bones must provide enough support. Indeed, in the case of an extinct animal, except for fossilized footprints and other tantalizing evidence of behavior, anatomy is

all we have to work with, at first. Yet that does not mean that behavior cannot be addressed by indirect scientific means.

Here we use two intertwined case studies from our research on animal limb biomechanics, one on extinct dinosaurs and another on extant elephants, to illustrate how anatomical methods and evidence are used to solve basic questions. The dinosaur study is used to show how biomechanical computer modeling can reveal how extinct animal limbs functioned (with a substantial margin of error that can be addressed explicitly in the models). The elephant study is used to show how classical anatomical observation and three-dimensional (3D) imaging have powerful synergy for characterising extant animal morphology, without biomechanical modeling, but also as a first step toward such modeling.

We focus on how a combination of classical techniques (particularly dissection, osteology, and functional anatomy) and modern techniques (especially imaging and computer modeling) are integrated to reveal how limbs function, and how anatomy is related to behavioral analyses such as biomechanics. We hope that this might inspire other functional biologists, clinicians, or researchers in other disciplines to see how an integration of anatomical methods can yield exciting insights into animal function or behavior.

¹Structure and Motion Laboratory, Department of Veterinary Basic Sciences, The Royal Veterinary College, University of London, Hatfield, Hertfordshire AL9 7TA, UK, and ²Leibniz Institute for Zoo and Wildlife Research (IZW), Berlin, Germany

3.2 Example 1: The Dinosaur *Velociraptor mongoliensis* Osborn 1924

Velociraptor (e.g., of *Jurassic Park* media fame) is a member of the theropod dinosaurs: habitually bipedal, ancestrally carnivorous animals that include living birds (e.g., Gauthier 1986; Sereno 1999). It is a Late Cretaceous representative of the closest known relatives of all birds: the deinonychosaurs. Although it is a late branch of this lineage and slightly large (<25 kg; e.g., Hutchinson 2004b) compared with earlier members (e.g., *Micro-raptor*; Xu et al. 2003) it is useful for understanding the evolution of traits present in extant birds, such as crouched striding bipedalism or the functions of homologous muscles in standing and moving (e.g., Gatesy 1990; Carrano 1998; Hutchinson and Gatesy 2000). As a model of the contemporary *Tyrannosaurus rex*, from a phylogenetically more distant lineage of theropods, is available (Hutchinson et al. 2005), we had a guide for how to construct this model and also a second extinct taxon to which we could compare the mechanics of homologous muscles.

We used a Cyberware 3030 3D color laser digitizer (Cyberware, Inc., Monterey, California, USA) to capture the 3D surface geometry of the pelvis and hindlimb of two similarly-sized specimens (Institute of Geology, Mongolia specimens IGM 100/986 and 100/985). Neither was 100% complete and intact, so we had to scale elements from the better-preserved pelvis of the smaller specimen (IGM 100/985) to match the larger, by using linear measurements (lengths and heights) of the two to establish proportional transformations. After we filled any holes and deformations were corrected for the best-preserved right or left elements, we ‘mirrored’ these elements about their midline axis in order to create the element of the opposite side of the limb. Although we created a left limb (and left half of the pelvis) for simplicity here we focus only on the single right limb and right side of the pelvis. Unlike elephants, *Velociraptor* was habitually bipedal, so we do not focus on its forelimb anatomy and mechanics here. We took additional measurements of the tail and other adjacent body parts to aid placement of soft tissues even though these elements were not included in the model.

We articulated these 3D images of our composite *Velociraptor* into a poseable skeleton in SIMM

musculoskeletal modeling software (Musculographics, Inc.; Chicago, IL) following the methods of Hutchinson et al. (2005). Briefly, we used hemispheres centered on the acetabulum and femoral head to calculate the geometric origins (0,0,0 in x,y,z coordinates) of the pelvis and femur segments to articulate them. We calculated the approximate geometric origins of the femoral condyles, tibial malleoli, and distal metatarsal condyles in order to establish the mean centers of joint rotation of their respective segments (tibiotarsus, metatarsus, and pes) as well. The lengths of the femur, tibia, and metatarsus were increased by 7.5%, 5%, and 10% to account for missing soft tissue between bony joint surfaces (Hutchinson et al. 2005). These procedures allowed articulation of the skeleton in the software (Fig. 3.1). Manual manipulation of joint orientations allowed us to check whether the movements of the segments were realistic throughout the ranges of motion allowed in the model, which were assessed by examination of the original material to bound ranges of feasible joint flexion/extension, ab/adduction, and lateral/medial rotation.



FIG. 3.1. Articulated right hind limb of *Velociraptor mongoliensis* in musculoskeletal modeling software, in lateral view. The pose shown is an arbitrary one; the reference pose was with all bones above the foot fully vertical.

Subsequently, we used muscle scars and comparison with dissections of extant relatives of *Velociraptor* (birds, crocodylians and other Reptilia) to reconstruct the hindlimb musculature of the right leg, following Hutchinson (2001a,b, 2002; Hutchinson and Gatesy 2000; Carrano and Hutchinson 2002). We then added curved wrapping surfaces to guide muscles on more realistic non-linear 3D paths, again using the skeletal anatomy and extant taxa as a guide (Hutchinson et al. 2005). Once we checked these muscle attachments to ensure no anomalous results occurred (e.g., sudden jumps or loops of the muscle-tendon unit paths as joints were moved), the model was ready (Fig. 3.2).

Here we focus on the relationships of muscle moment arms (see An et al. 1984; Delp et al. 1999) to joint angles (as per Hutchinson et al. 2005) for the major flexors and extensors of the hip joint, as these muscles are presumed to have undergone the most dramatic anatomical and functional transformations between the common ancestors of tyrannosaurs (basal coelurosaurian theropods; distant from birds) and deinonychosaurs (eumaniraptoran theropods; sister group [i.e., cousin lineage] to birds). We compared our model of *Velociraptor* with a model of *Tyrannosaurus* (Hutchinson et al. 2005), with muscle moment arms normalised by a reference bone length to

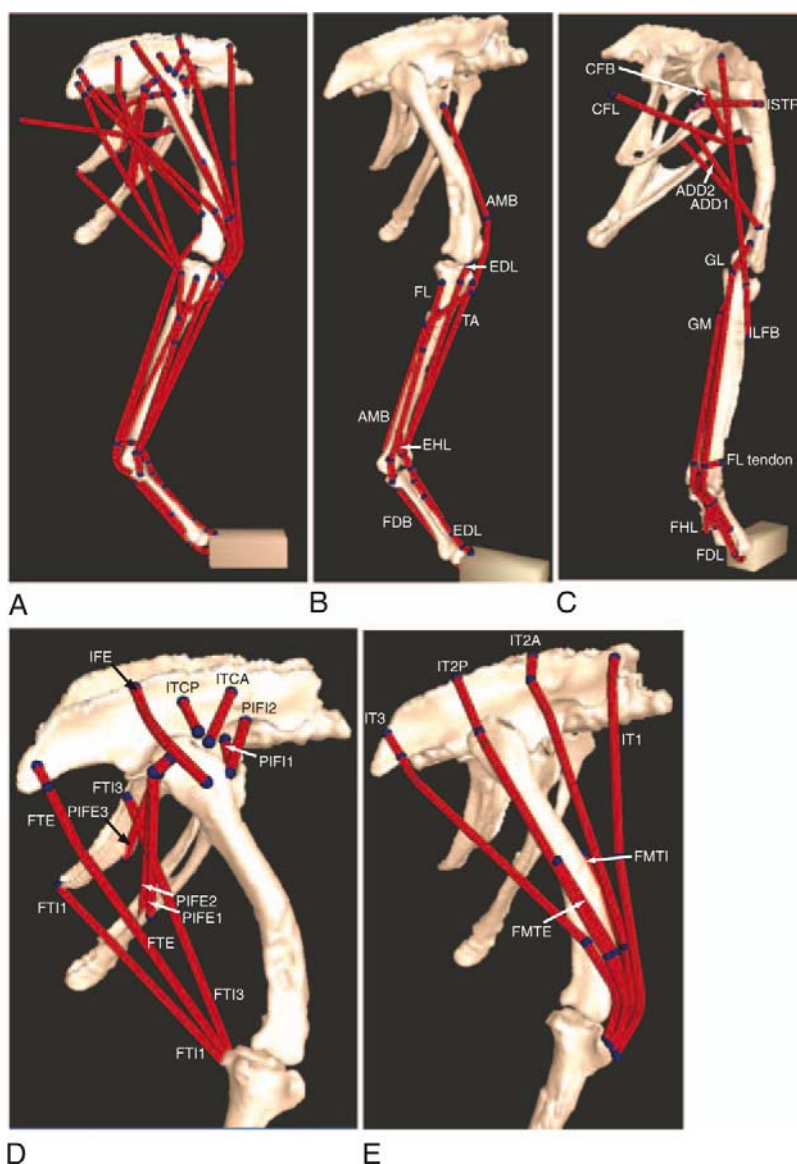


FIG. 3.2. Muscles (red lines) of *Velociraptor* right hind limb model, in lateral view with all shown (A), oblique cranio-lateral view of lower limb muscles (B), oblique caudolateral view of some hip extensor and lower limb muscles (C), dorsolateral view closeup of hamstring (flexor cruris complex), external puboischiofemoral, and deep dorsal thigh muscles (D), and cranio-lateral view closeup of *M. iliotibialis* and *M. femorotibialis* knee extensor muscles (E). See Table 3.2 for muscle abbreviations (see Color Plates, Fig. 3.2).

TABLE 3.1. Reference lengths of segments (from musculoskeletal model) used for normalizing moment arm measurements. The ‘Ratio’ column shows the ratio of the length in *Tyrannosaurus* to the corresponding length in *Velociraptor*.

Length	<i>Velociraptor</i>	<i>Tyrannosaurus</i>	Ratio
Femur	0.160	1.22	7.63
Tibiotarsus	0.221	1.27	5.75
Tarsometatarsus	0.120	0.780	6.50

remove the confounding effects of body size. For muscles acting about the hip joint, the femur length (hip to knee joint distance) was used as the reference length; for muscles acting about the knee, the ‘tibiotarsus’ length (knee to ankle joint), and for muscles acting about the ankle and toes, the ‘tarsometatarsus’ length (ankle to metatarsophalangeal joint). Table 3.1 shows these values for *Velociraptor* and *Tyrannosaurus*.

3.3 Example 2: Asian Elephants (*Elephas maximus* Linnaeus 1758)

As elephant anatomy is poorly understood and access to specimens is severely difficult due to their protected conservation status, low mortality rates and population sizes, remote locations, and size (e.g., handling, transport, and storage logistics), making the most of available specimens is a high priority for our research. Dissection of course renders cadaveric specimens unusable for other analyses such as *in vitro* mechanical testing, so we conventionally collect 3D imaging data with computed tomography (CT) and magnetic resonance imaging (MRI; not shown here) when possible before dissecting specimens, in order to preserve as much anatomical data as possible. Such data are also invaluable for constructing computer models such as the example above, so imaging has much value. Here, we focus on what we learned about elephant limb anatomy from 3D imaging (CT) combined with conventional dissection.

We obtained the fore and hind limbs (separated from the torso/pelvis, with most extrinsic musculature attached) of an adult female (~25 years old; 3400 kg body mass) from Whipsnade Wild Animal Park (Bedfordshire, UK). This animal was euthanised for severe arthritis and osteomyelitis in the left hindlimb; we obtained the right limbs which appeared to be in reasonably sound musculoskel-

etal condition, although we make some notes on evident pathologies below.

We did CT scanning on a Picker PQ5000 station (General Electric Company, Coventry, UK), with typically 150 axial x-ray slices at 1.5–5 mm intervals (depending on specimen size), 512 × 512 pixels, 120 kVp and 200 mA intensity. After imaging, we loaded the raw DICOM format scanner images into MIMICS 10.1 (Materialise, Inc; Leeuwen, Belgium) software where we used gray-value thresholding to identify tissues of different densities (e.g., muscle, tendon, and bone) and create 3D images of each identified structure (Fig. 3.2). These 3D models are the main subject of this part of the study.

After imaging, we quickly dissected all segments and stored them in a freezer (–20°C) or cold room (4°C) when not in use. Abundant digital photos and video were taken as supplementary documentation during dissection. We used supplementary cadaver data (collected in the same fashion) from the complete fore and hindlimbs of one neonatal, one juvenile and one adult Asian elephants plus a total of (including from the complete limbs) 5 adult and 4 juvenile/neonatal manus, and 4 adult and 4 juvenile/neonatal pedes (of which one manus was an African adult, and one pes was an African juvenile), plus dry museum bone specimens (from the Cambridge Museum of Zoology and Royal Veterinary College Anatomy Museum) to compare with our main specimen in order to assess individual variation or pathology.

Additionally during the dissections we collected data on the muscle-tendon unit architecture of all limb muscle groups, following Payne et al. (2004, 2005) and references therein. This included muscle and tendon masses and lengths, and muscle fascicle lengths and pennation angles, with which muscle force production can be estimated (e.g., Alexander et al. 1981; Zajac 1989; Alexander and Ker 1990; Payne et al. 2004, 2005). We do not focus on these data here, but they are essential anatomi-

cal data needed for biomechanical analysis and few such data exist for most extant taxa. A comprehensive, quantitative anatomical study would include all such measurements in addition to traditional origins, paths, and insertions.

Here, we focus mainly on the osteological anatomy of Asian elephants (which unlike *Velociraptor* or African elephants, is not well described in the literature), using our adult female specimen as a primary example but with ancillary data from other specimens as noted above, and soft tissue data where most relevant for interpreting the osteology.

3.4 Results

3.4.1 *Velociraptor Model*

Absolute values for hip muscle moment arms in the sagittal plane are in Table 3.2. Generally the model's flexor and extensor muscle moment arm patterns (Figs 3.3,3.4) matched those of *Tyrannosaurus* (Hutchinson et al. 2005). For the hip flexor and extensor muscles, most muscles had relatively larger moment arm values in *Tyrannosaurus*. Some relative magnitudes were still strikingly dif-

ferent, however: the deep dorsal thigh muscles (*M. iliotrochantericus caudalis* and *M. puboischiofemoralis internus*; both parts of each group) showed reduced hip flexor moment arms and switches between hip flexor and extensor moment arms in relatively extended femoral orientations in *Velociraptor*, unlike in *Tyrannosaurus* (Fig. 3.4). In contrast, *M. flexor tibialis internus 1* (dubiously present; Carrano and Hutchinson, 2002) had relatively larger moment arms in *Velociraptor* (Fig. 3.3E). *M. puboischiofemoralis externus 1* and 2, whose origins were rotated caudally in maniraptoran theropods with retroversion of the pubic bones, showed relatively much lower moment arms for hip flexion, but still were competent hip flexors. Lower limb muscles were relatively similar between the two taxa, which is consistent with the observation that lower limb anatomy did not transform as drastically between basal coelurosaurs and eumaniraptoran theropods (e.g., Hutchinson 2002).

3.4.2 *Elephant Models*

Our rendered 3D models of elephant limb bones were of a high enough resolution that all major

TABLE 3.2. Muscle moment arm results for *Velociraptor* model. Muscle names, abbreviations, and moment arms at 0° and 45° hip joint angles (larger values are more flexed; 0° is a femur held perpendicular to the pelvic axis), and minimum, maximum, and mean values are shown. Moment arm units are in centimeters; negative moment arms are hip flexor whereas positive are extensor.

Muscle	Abbrev.	At 0°	At 45°	Min	Max	Mean
<i>M. iliotibialis 1</i>	IT1	-6.6	-4.8	-8.4	-4.8	-6.8
<i>M. iliotibialis 2, preacetabular</i>	IT2A	-4.0	-4.2	-4.2	-3.8	-4.1
<i>M. iliotibialis 2, postacetabular</i>	IT2P	-0.38	-0.65	-0.65	-0.29	-0.37
<i>M. iliotibialis 3</i>	IT3	5.4	6.0	3.3	6.1	5.0
<i>M. ambiens</i>	AMB	-3.1	-4.1	-4.1	2.6	-1.8
<i>M. iliofibularis</i>	ILFB	3.6	4.3	3.2	4.3	3.6
<i>M. iliofemoralis externus</i>	IFE	0.40	1.1	-1.9	1.1	-0.25
<i>M. iliotrochantericus caudalis, anterior</i>	ITCA	-1.3	-1.6	-1.6	0.87	-0.80
<i>M. iliotrochantericus caudalis, posterior</i>	ITCP	-1.4	-1.6	-1.5	0.59	-0.93
<i>M. puboischiofemoralis internus 1</i>	PIFI1	-2.3	-1.6	-2.6	-1.6	-2.3
<i>M. puboischiofemoralis internus 2</i>	PIFI2	-2.4	-2.0	-2.4	1.7	-1.5
<i>M. flexor tibialis internus 1</i>	FTI1	10	-2.4	-2.4	11	8.0
<i>M. flexor tibialis externus</i>	FTI3	3.0	0.39	0.39	3.5	2.7
<i>M. flexor tibialis internus 3</i>	FTE	6.4	4.3	4.3	7.3	6.5
<i>M. adductor femoris 1</i>	ADD1	3.9	-1.1	-1.1	5.0	3.4
<i>M. adductor femoris 2</i>	ADD2	3.9	0.25	0.25	4.4	3.4
<i>M. puboischiofemoralis externus 1</i>	PIFE1	-0.77	-1.7	-1.7	0.13	-0.70
<i>M. puboischiofemoralis externus 2</i>	PIFE2	-0.70	-1.4	-1.4	0.12	-0.58
<i>M. puboischiofemoralis externus 3</i>	PIFE3	-0.39	-0.66	-0.66	0.37	-0.24
<i>M. ischiotrochantericus</i>	ISTR	0.43	-0.41	-0.41	0.76	0.39
<i>M. caudofemoralis brevis</i>	CFB	4.5	4.5	3.0	4.7	4.1
<i>M. caudofemoralis longus</i>	CFL	4.4	3.2	3.2	5.9	4.7

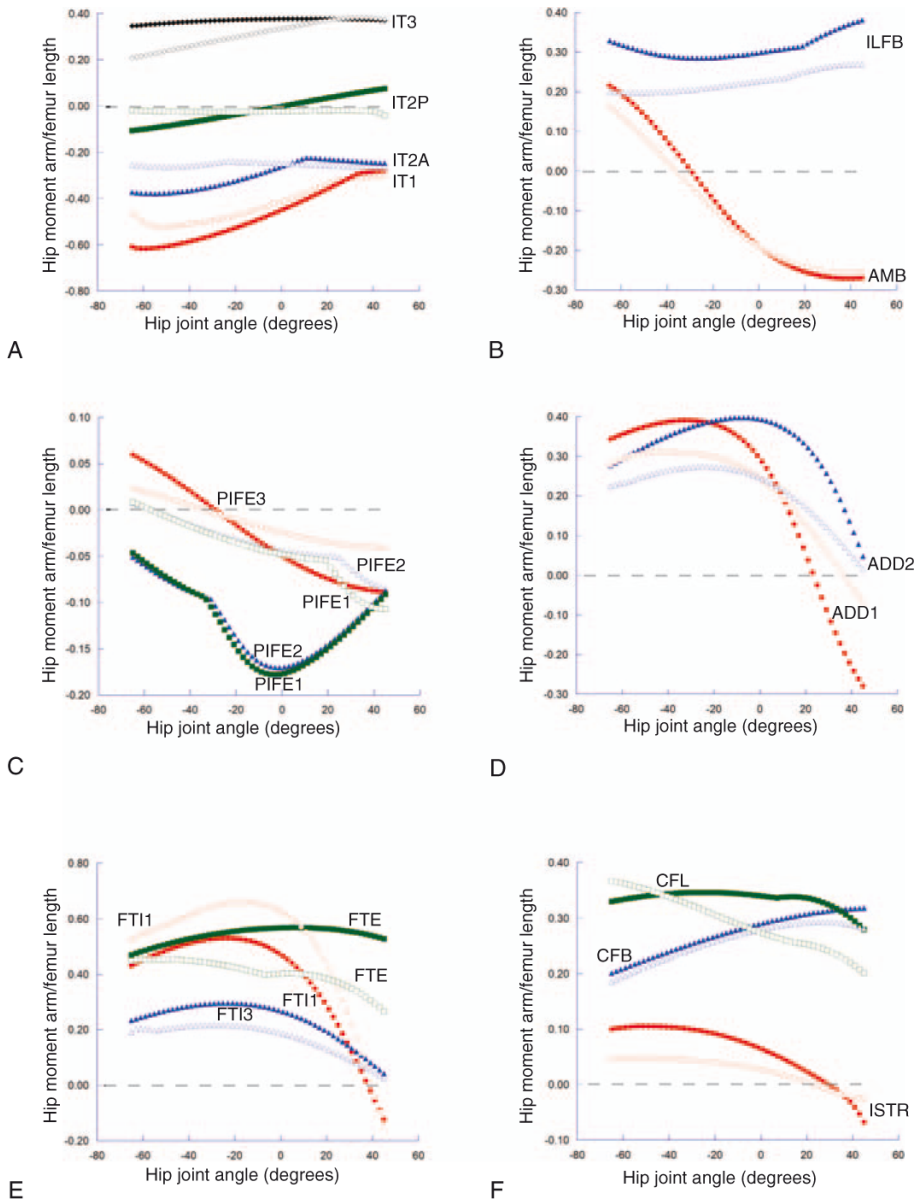


FIG. 3.3. Hip flexor/extensor moment arm-hip joint angle relationships for major hip muscles in *Velociraptor* (open symbols) and *Tyrannosaurus* (filled symbols). Moment arms are normalized by femur length (see text and Table 3.1) for size-independent comparisons. Positive moment arms are extensor; negative are flexor. A hip joint angle of 0° represents a vertical femur; negative values are extension past that point and positive values are flexion (femoral protraction). **A**, M. iliobtibialis 1 – 3 (IT1 – 3). **B**, M. iliofibularis (ILFB) and M. ambiens (AMB). **C**, Mm. puboischiofemorales externi 1 – 3 (PIFE1 – 3). **D**, Mm. adductores femorii 1 + 2 (ADD1 + 2). **E**, Mm. flexores tibiales interni 1 + 3 (FTI1 + 3) et externus (FTE), and **F**, M. ischiochantericus (ISTR) and Mm. caudofemorales brevis et longus (CFB, CFL) (see Color Plates, Fig. 3.3).

anatomical features of the bones – even subtle muscle scars – described in the excellent osteological studies by Smuts and Bezuidenhout (1993, 1994) could be identified in our main specimen and other elephants we studied. We found few striking osteological differences between the literature descriptions of African elephants and our

Asian elephants. Our specimens showed the same sexual dimorphism observed by the latter authors (e.g., more prominent muscle scars in female elephants; surprising considering the larger mean size of males). We proceed from proximal to distal elements of the fore and hind limbs (Fig. 3.5), noting where our specimen (or any others)

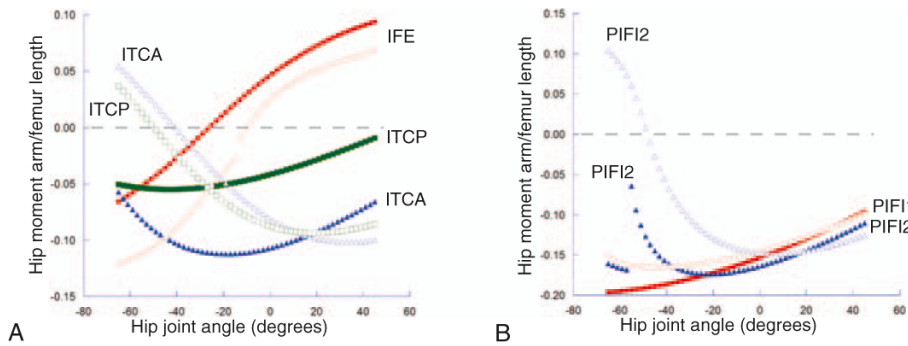


FIG. 3.4. Additional hip moment arm-joint angle relationships as in Fig. 3.3. **A**, *M. iliofemoralis externus* (IFE) and *M. iliotorchantericus caudalis* (ITCA, ITCP). **B**, *Mm. puboischiofemoralis internus 1 + 2* (PIF1 + 2) (see Color Plates, Fig. 3.4).

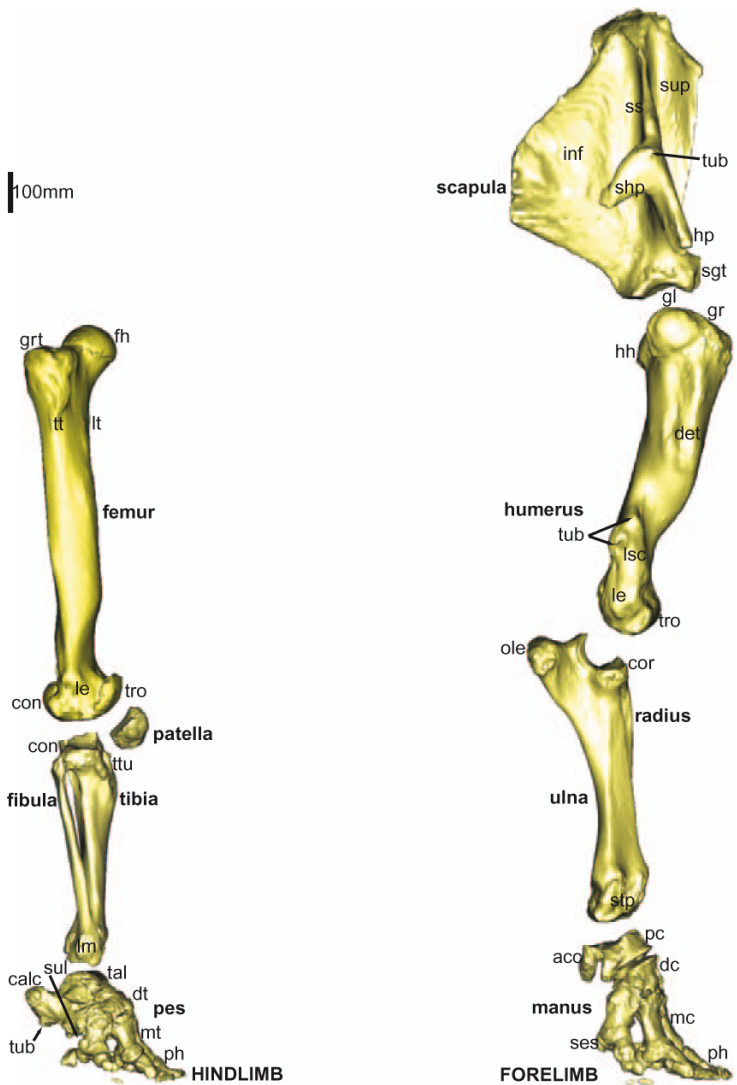


FIG. 3.5. Bones of the right fore and hind limb of our study specimen of *Elephas maximus*, three-dimensionally rendered in MIMICS software from CT scans. In lateral view. The major bones are moved slightly out of articulation so more of their surfaces can be seen. Abbreviations: acc = accessory carpal, calc = calcaneus, con = condyle, cor = medial coronoid process, dc = distal carpals (I-V), det = deltoid tuberosity, dt = distal tarsals (I-V), fh = femoral head, gl = glenoid surface, gr = greater tubercle, gtr = greater trochanter, hh = humeral head, hp = hamate process, inf = infraspinous fossa, le = lateral epicondyle, lm = lateral malleolus, lsc = lateral supracondylar crest, lt = lesser trochanter, mc = metacarpals (I-V), mt = metatarsals (I-V), ole = olecranon process, pc = proximal carpals (I-V), ph = phalanges (I-V), ses = sesamoid(s), sgt = supraglenoid tubercle, shp = suprahamate process, ss = scapular spine, stp = styloid process, sul = sulcus, sup = supraspinous fossa, tal = talus, tro = trochlear surface, tt = third trochanter, tub = tubercle, ttu = tibial tuberosity (see Color Plates, Fig. 3.5).

showed important differences from Smuts and Bezuidenhout's (1993, 1994) African elephant specimens. All bony epiphyses were fully fused except where noted; our main specimen was almost skeletally mature (Roth 1984).

The scapula had three tubercles on the scapular spine region: one midway along the lateral surface of the spine (part of *M. trapezius* insertion), a second on the spine at the juncture of the hamate and suprahamate processes (probable origin of fascial sheet extending down the forelimb), and a third on the lateral tip of the hamate process (end of deltoid partial origin, and attachment for cranio-lateral and cranial 'lacertus fibrosus' fascial sheets).

The humerus revealed two distinct features of the crista supracondylaris lateralis not noted elsewhere: there was one quite large tubercle (with a distal invagination) on the caudolateral side of the

crest near its proximal end (associated with the origin of *M. anconeus*), and then a second, smaller tubercle proximal to it on the crest (part of the *M. brachioradialis* origin).

The radius and ulna of our main specimen were fused together proximally quite strongly as well as partly fused at their distal articulation. The ulna had marked muscle scarring on the proximal half of the caudomedial surface of the corpus ulnae (*biceps brachii* partial insertion, as well as a second patch of scarring also visible in CT images on the proximal olecranon's caudolateral surface, distal to the tuber olecrani proper (part of the *M. anconeus* insertion).

The manus (Figs 3.5,3.6) showed strong ossification and rugosities but no evident pathology. We found no clear articulation of the ulnar carpal with metacarpal V – indeed, Smuts and Bezuidenhout's (1993) figures concur with this, unlike the text. The

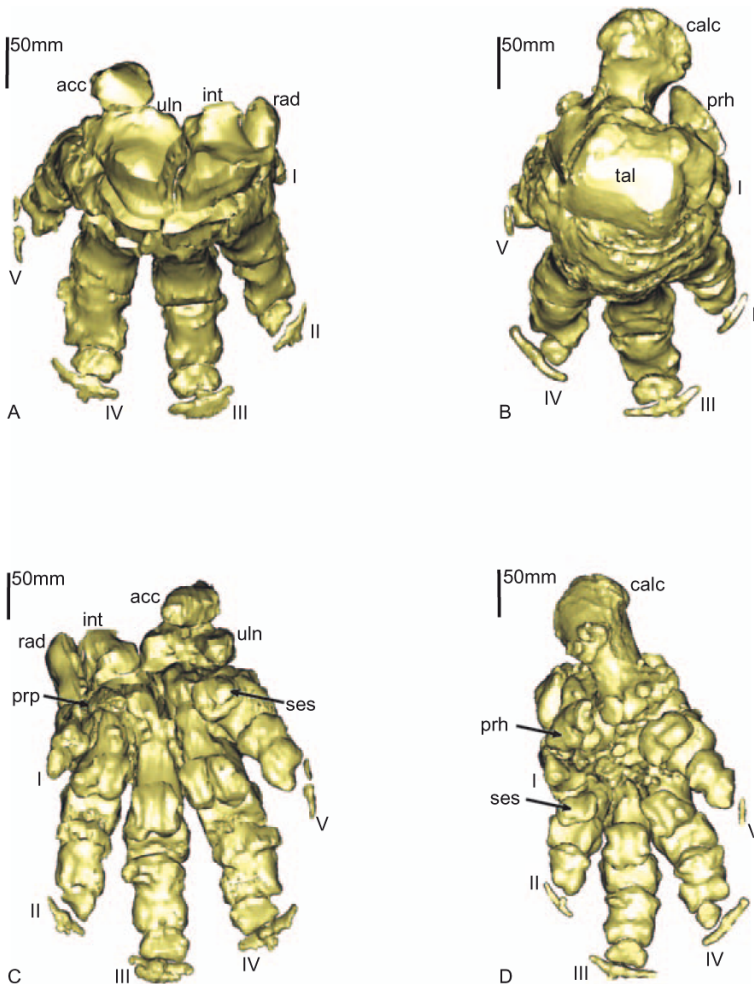


FIG. 3.6. Articulated bones of the right manus (A, C) and pes (B, D), in palmar (A, B) and planter (C, D) views. Abbreviations as in Fig. 3.5 caption plus: I-V = digits I-V, int = intermediate carpal, prh = prehallux, prp = prepollex, rad = radial carpal, tal = talus, uln = ulnar carpal (see Color Plates, Fig. 3.6).

accessory carpal was the normal insertion point for *M. extensor carpi ulnaris* (and *M. extensor digitorum lateralis*). Carpals 3 and 4 had plantar tuberosities, presumably for the insertion of *M. flexor carpi radialis*. The metacarpals match the descriptions of Smuts and Bezuidenhout (1993) very well, except that metacarpal II's proximal tuberosity was expanded proximally into a spine (this was not present in other individuals).

All manus digits except I had two large proximal sesamoids. Close examination of our main specimen showed at least one, maybe two ossifications in the location of the proximal sesamoid of digit I (Fig. 3.7A,B). However in our other five adult specimens we saw a single sesamoid in digit

I in two specimens, two separate sesamoids in one specimen, and an ambiguous number (one or two but resolution too coarse to determine) in the others. Juveniles tended not to have sesamoids visible at all in digits I and V. We infer that at least Asian elephants have two sesamoids in digit I, but they may fuse or be indistinguishable in adults.

In our main specimen, digit I of the manus had only one phalanx (although in two adult individuals we saw two phalanges), digits II-IV had the typical three phalanges (except one pathological adult individual only had two for each digit, and juveniles had anywhere from 2-3 identifiable phalanges, tending to increase with age as expected), and digit V had proximal and distal phalanges with a

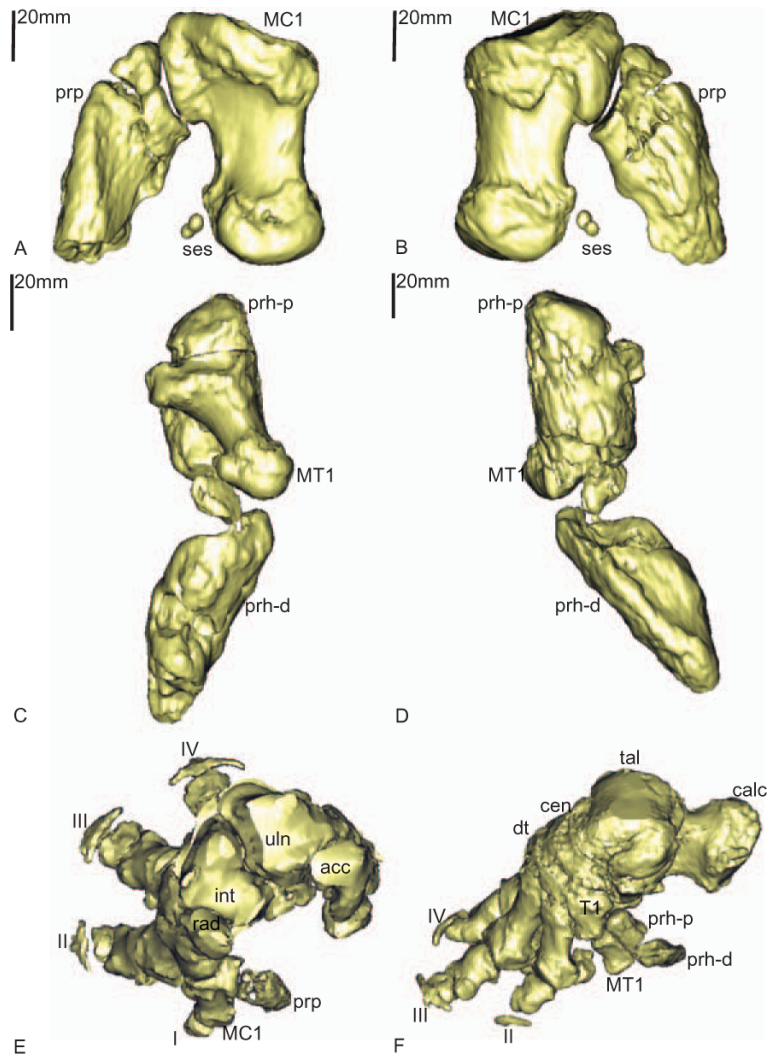


FIG. 3.7. 'Predigits' of the right manus and pes: prepollex in medial (A) and lateral (B) views, prehallux in cranial (C) and caudal (D) views, and dorsomedial views (not to scale) of manus (E) and pes (F), with articulations shown. Abbreviations as in Figs 3.5, 3.6 captions plus: cen = central tarsal, MC1 = metacarpal I, MT1 = metatarsal I, prh-d = distal segment of prehallux, prh-p = proximal segment of prehallux, T1 = (distal) tarsal I (see Color Plates, Fig. 3.7).

gap separating them (i.e., no ossified middle phalanx; contrary to the findings of Smuts and Bezuidenhout (1993), who found no ossified ungual). On closer investigation of the CT images, there appeared to be a cartilaginous middle phalanx of digit V that had failed to ossify in our main specimen, and this was likewise common but individually variable in other Asian elephants – two of our larger adult individuals even had a complete set of three ossified phalanges. Digits III and IV had ungual (distal) phalanges that, unlike the specimens described by Smuts and Bezuidenhout (1993), had articulations evident with the middle phalanges, whereas digit II had the usual gap between these two distalmost phalanges. These two patterns were variably present in other specimens. Digit V's ungual phalanx was divided into medial and lateral halves; likewise variable even among adults. Below we add additional notes on the anatomy of the prepollex.

We observed no other external features of the femur, patella, tibia, or fibula (Fig. 3.5) that Smuts and Bezuidenhout (1994) did not already point out, except some pathologies noted below for our main specimen. Likewise we saw the same details that the latter authors note; there were no marked osteological differences between their African and our Asian elephants. The tibial epiphysis was incompletely fused, unlike the other limb bones; although this is slightly unusual for typical elephants (Roth 1984) we assume that it is merely individual variation rather than pathology.

Some details of pes osteology (Figs 3.5,3.6) in our main specimen were obscured by some extraordinary pathologies (described further below), yet the basic anatomy of elephant pedes was still recognizable, especially distally. The calcaneus had marked ligamentous and tendinous scarring, including on the plantar surface of the calcaneal tuber, corresponding to the adductors and abductors of digit V. Additionally, there was a strong lateral tuberosity at the base of the tuber, caudal to the articulations with metatarsal V and tarsal IV. This tuber also bounds a tendinous sulcus with a hooklike project of the caudolateral base of the articular surface for metatarsal V; this sulcus is for the tendon of *M. tibialis caudalis*. Talus and distal tarsal anatomy was also as described by Smuts and Bezuidenhout (1994), with all major details visible except where obliterated by pathological fusion or osteophytes. The pes had the typical five metatarsal bones, conforming quite

well to the description by Smuts and Bezuidenhout (1994). Pathologies, especially proximally, are noted below.

As in African elephants, the hallux (digit I) had only one very small, flat proximal sesamoid (lying between the metatarsal trochlea and the prehallux; described below) and no phalanges. This was variable in our eight other specimens – adults and immature elephants alike had either zero or one sesamoid. Curiously, all five of our adult specimens lacked hallucal phalanges whereas all four juveniles had one phalanx, so phalanx number is either individually or ontogenetically variable (our sample size is too small to determine). The other digits each had two proximal sesamoids (none fused as Mariappa 1986 claimed for digit II).

Digits II and V had two ossified phalanges, lacking a middle phalanx – the proximal and distal (ungual) phalanges were separated by a gap where a presumably cartilaginous nodule represented the middle phalanx. However this pattern differed in adults: three complete digits were present in digit II in the four other individuals, whereas half had either two or three phalanges in digit V. Juveniles had two ossified phalanges in digit II and 1–2 in digit V. The unguals of these two digits were typically simple and crescent-shaped; ungual II had a hooked ventromedial tuberosity, whereas ungual V lacked any marked tuberosity in our main specimen, and this shape was likewise variable among other specimens. Digits III and IV usually had the usual full complement of three phalanges in adults (but one had two phalanges in digit IV), whereas juveniles had 2–3. If an elephant had three phalanges in any one digit, it was always digit III. The ungual of digit III had a tuberosity that was offset slightly medially (unlike in typical African elephants), whereas the tuberosity on digit IV was markedly reduced, and the middle phalanx was much smaller than in digit III. However, this asymmetry was not typical for other specimens.

Our CT images of our main specimen and others showed some remarkable features of the fore and hind feet that deserve greater attention, so we focus on these here. From our observations of the feet of four African elephants (from juvenile to adult) we are confident that these comments apply to both major species of elephants. The anatomy of the bizarre 'predigits' (prepollex and prehallux; digit-like structures of unknown composition or

ontogeny that lie medial to digit I) of elephant manus and pedes caused some confusion in early literature concerning the number of digits in elephants (see Smuts and Bezuidenhout 1993, 1994). This anatomy has not previously been described in detail, nor has its ontogenetic variation been inspected. As CT scanning provides noninvasive anatomical data on the *in situ* positions and structure as well as relative density (i.e., calcification) of these mysterious elements, here we add detailed description.

The prepollex (Fig. 3.7A,B,E) is a single segment (in all specimens) that articulates only with metacarpal I. It is claw or hook-shaped, with the concave surface of the hook oriented craniomedially. Its articulation is a large rugose, convex boss on the proximal caudal (plantar) surface of metacarpal I, forming a saddle-shaped joint articulation with the concave, crescent-shaped proximal surface of the prepollex. The prepollex has a longitudinal ridge on its caudolateral and craniomedial surfaces.

The prehallux (Fig. 3.7C,D,F) is a slightly curved, rodlike structure that articulates with tarsal I and metatarsal I, on their caudal (plantar) surfaces. The prehallux consists of at least two and sometimes three calcified segments (variable among specimens; Neuville (1935, fig. 26) showed four possible centers of calcification) that have an articulation at the level of the distal end of metatarsal I. A concave notch is present on tarsal I that a rounded peg on the proximal segment of the prehallux fits into, approximating a ball-and-socket joint. This prehallucal segment then lies parallel to metatarsal I and sits appressed to a flat caudomedial groove in that bone (Fig. 3.7F). The nature of the bones surrounding it, especially tarsal I's main articulation with it, is that the movements of the prehallux are restricted to a dorso-caudal plane.

Both 'predigits' calcify (or ossify; histological data are needed to test this) throughout growth, with the calcification of cartilages proceeding from proximal and distal toward the middle, and from the surfaces inward toward the core, with a tendency for thicker calcification on the lateral sides.

We also observed interesting pathologies in our primary female specimen that we are not aware of ever having been described in elephants, even though the disorders (osteomyelitis and osteoarthritis, primarily) they are symptoms of are major

causes of mortality in captive elephants (Csuti et al. 2001). These pathologies were centered around the tarsus (Figs 3.5,3.6). The distal end of the tibia (caudal side of the cochlea tibiae) had extended further distally behind the talus, forming a prong that stiffened the back of the ankle joint. Likewise the distal fibula showed excessive growth, and the talus had enlarged proximal articular facets, especially laterally. The tarsals show other pathologies related to decreasing the mobility of the ankle joint complex. The distal tarsals (centrale and tarsals I-IV) were largely fused to each other, sharing marrow cavities. Likewise, the medial and distal surfaces of the calcaneus was fused to the talus, centrale, and tarsal IV. Generally, the surfaces of all tarsals was roughened by this ankylosis and scarred with pits, vascular channels, and osteophytes (spurs). This pathology extended into the proximal metatarsals, with signs of fusion particularly between metatarsal V and tarsal IV, and metatarsal I and tarsal I. The tuberosities at the bases of the metatarsals were larger than normal, presumably related to this pathology. On the cranial (dorsal) base of metatarsal III there was an erosive channel penetrating through the bone.

3.5 Discussion

Our examples show how anatomy remains a discipline of fundamental importance, for example in biomechanical analysis, and how anatomical analysis has evolved with and been enriched by new imaging technologies.

3.5.1 *Velociraptor Model*

Velociraptor is more closely related to extant birds than is *Tyrannosaurus* (e.g., Gauthier 1986; Sereno 1999), the other dinosaur for which muscle moment arm-joint angle relationships have been estimated (Hutchinson et al. 2005). Although both are Late Cretaceous terminal taxa within long-lived lineages (deinonychosaurs and tyrannosauroids, respectively); both dating back to at least the Late Jurassic (Sereno 1999; Xu et al. 2003) and have lost some ancestral features of those lineages and gained some derived features (especially larger size), they still have the potential to reveal anatomical and functional transitions within the hind-limb along the line from coelurosaurian dinosaurs to extant birds. This is particular true for those

anatomical details that are retentions of features that are ancestral along this line (e.g., Gatesy 1990; Carrano 1998; Hutchinson and Gatesy 2000), despite the distance of the terminal taxa from the line itself. Hence as long as one is cautious about the relative antiquity of features in such terminal taxa (by using proper outgroup analysis and considering more/less primitive traits in related taxa that are not modelled), biomechanical models of these taxa can still reveal the evolutionary polarity of functional traits.

Many hip muscles showed relatively larger moment arms (even with size factored out) in *Tyrannosaurus*. This was likewise generally the case for distal muscle groups including the knee, ankle, and toe extensors and flexors (not shown). This matches the expectation of some positive allometric scaling of muscle moment arms from smaller to larger theropods (e.g., Alexander et al. 1981; Biewener 1989, 1990; Hutchinson 2004b; Hutchinson et al. 2005) – larger moment arms are needed to maintain similar peak stresses on the musculoskeletal system during the support of body weight or protraction of relatively heavier limb segments. However more data from other extant and extinct theropod taxa are needed to test whether this is actually allometric scaling or differences in phylogenetic position. In particular, the shortened postacetabular ilium (and reduced tail) of maniraptoran theropods (e.g., Xu et al. 2003) might explain the smaller hip extensor moment arms for most muscles originating from there.

The more unusual results of the *Velociraptor* model when compared with *Tyrannosaurus* can partly be explained by phylogenetic differences in anatomy between basal coelurosaurs (e.g., tyrannosaurs) and maniraptoran theropods (e.g., deinonychosaurs). *Velociraptor* has the shortened but somewhat more strongly retroverted ischia typical of its clade, which should have moved some muscle origins further caudally and transformed their moment arms. Our model does show some relatively increased moment arms for some but not all muscles with ischial (e.g., M. flexor tibialis internus 1 if present) origins. Likewise, shape changes of the preacetabular ilium and lesser trochanter/trochanteric crest in maniraptorans might explain the altered moment arms for the deep dorsal thigh muscles (Fig. 3.4) attaching to those surfaces (Hutchinson 2001a,b; Carrano and Hutchinson, 2002) in *Velociraptor*, relative to *Tyrannosaurus*.

Researchers have long discussed the effects of retroversion of the pubic bones in maniraptorans (and convergently in ornithischian dinosaurs) on thigh muscle function (e.g., Romer 1927; Walker 1977; Perle 1985; Hutchinson and Gatesy 2000). Rather than resulting in a dramatic transformation of the functions of the major pubic muscles Mm. puboischiofemorales externus 1 and 2, our models show that this change only reduced (but did not eliminate as Hutchinson and Gatesy (2000) inferred, although this might have occurred deeper within the bird lineage) their hip flexor moment arms. A functional shift into hip extension (i.e., femoral retractors; Romer 1927; Charig 1972; Perle 1985), not flexion, is strongly rejected by the model. This conservation of hip flexor function results from the insertion of these muscles, which is still laterally positioned on the proximal femur (e.g., Hutchinson 2001b), and lies above, not below, the femoral head (*contra* Perle 1985), hence imparting a flexor moment arm to the muscle group. This very likely holds for ornithischian dinosaurs as well.

The ultimate explanation for retroversion of the pubes remains elusive – shifts of the body's center of mass and sizes or positions of digestive or respiratory tissues, for example, are at least consequences of this retroversion, but we remain agnostic about evolutionary causation (see also Hutchinson and Gatesy 2000).

3.5.2 Elephant Models

We were impressed to see in our elephant specimens how fine osteological details first described from visual observation of dried museum skeletons (e.g., Blair 1710; Smuts and Bezuidenhout 1993, 1994) could still be clearly observed with conventional CT scanners. This imaging approach also spares the considerable effort of thoroughly cleansing and degreasing bones, which often damages them. In the case of heavy elephant bones, this also renders sharing these anatomical data with other researchers much more simple than sharing the actual specimens. Furthermore, the detailed anatomy of the prepollex and prehallux has surely been obscured (e.g., see review in Eales 1929) by the emphasis of anatomists on describing cleaned osteological specimens, from which less ossified (and perhaps unexpected) structures such as these 'predigits' can easily be overlooked or lost. Modern imaging techniques

help ensure that such strange calcifications are recognized and described *in situ*. In particular, the soft tissue context in which they are embedded can be analysed before destructive dissection.

The finding that elephant prepollices and prehalluces have identifiable osteological correlates (e.g., Witmer 1995) of their articulations with other bones of the manus and pedes opens the possibility that the evolutionary history of these strange 'sixth digits' of elephantids can be traced through the fossil record. As these neomorphic digits are unknown in extant relatives (e.g., sirenians and hyraxes), they must have arisen within the Proboscidea. Presumably, as they support the digital cushions of subunguligrade elephant feet (Weisengruber et al. 2006), they originated in concert with the expansion of these digital cushions into the highly derived footpad structure of elephantids. Hence any information on the presence/absence of the articular surfaces in fossils would not only illuminate when the prepollex or prehallux first evolved, but also shed light on the genesis of this remarkable footpad.

We also have described numerous osteological correlates of soft tissue attachment in elephant limb bones that are useful for functional morphologists and paleontologists, and add biological context to characters useful in systematic studies. These features seem to be consistent between Asian and African elephant species, yet individual variation in many of these features remains very poorly understood. Quite a few of them are expressed at a very young age (e.g., Mariappa 1986).

How many toe bones do elephants have? There were no differences among the numbers of digits (five total in each manus and pes) in our specimens; we expect that deviations from this pattern are highly abnormal for any elephants. We found some different counts of phalanges and sesamoids in the manus and pes than sometimes reported for elephants. In the manus, authors seem to agree on a proximal sesamoid count of 1-2-2-2-2 but we found that there are two proximal sesamoids associated with digit I, albeit very small ones that may sometimes be co-ossified. We found that the manus phalangeal formula is 1-3-3-3-2 for Asian and African elephants (Smuts and Bezuidenhout 1993; Ramsay et al. 2001), but two of our seven adult Asian elephants had an extra digit I phalanx. Eales (1928, 1929) had similar findings for a fetal African elephant with a phalangeal formula of 2-3-3-3-2.

Sikes (1971) indicated a manus phalangeal formula of 1-2-2-2-2 for African elephants; apparently the distal phalanges of digits II-IV were overlooked, or variability is even higher than suspected.

Pes digit I had no phalanges in adults, unlike our juvenile specimens, which match the fetal Asian elephant that Mariappa (1986) described as having one phalanx that was 'a minute cartilage' (p.27). Interestingly, Eales (1928, figs 6-8) showed two phalanges here in a fetal African elephant, although her various figures (e.g., 1928, figs 19-22) do not always show consistent phalangeal counts for other digits and her text (1929) contradicts this. It seems likely that the 'fused sesamoids' Mariappa (1986) noted for digit II were too small in his fetal specimen to differentiate; adults typically have two separate ossifications (*vide* Ramsay et al. 2001). If this is correct, then African and Asian elephants both typically should have a pedal sesamoid count of 1-2-2-2-2 (Smuts and Bezuidenhout 1994; Ramsay et al. 2001) although some individuals lack the hallucal sesamoid (none seem to have paired ones). Mariappa (1986) claimed three phalanges in digit II but only two phalanges in digit IV for a fetal Asian elephant. It is possible that Mariappa (1986, p. 26) referred to digit IV where digit V was intended; this matches his figure 1.17. We found the opposite in our main specimen, although this was variable among our other adults – a phalangeal formula of (0/1)-3-3-3-3 is common although some individuals, even large adults, have two phalanges for some of digit(s) II-V (although never digit III if other digits have three phalanges). Sikes (1971) again stated a phalangeal formula of 1-2-2-2-2 for the pes, which seems an oversimplification of the general pattern. Neuville (1935, figures 17,18) showed an unusual pes specimen with a possible fourth phalanx for digit III.

The patterns we have found for manus and pedal anatomy are from multiple individuals of a wide size and age spectrum. These generally match the observations for African elephants (Smuts and Bezuidenhout 1993, 1994), although differences in manual phalangeal count (e.g., manus digit I) probably also relate to misidentification of phalanges (as middle/ungual) due to the study of non-articulated cleaned bones, rather than the *in situ* specimens we have observed. Additionally, the emphasis on studying fetal or otherwise immature specimens (inevitably with less ossification and more ambiguous differentiation of morphology) has been misleading. We conclude that there are

no salient differences in phalanx or sesamoid number between the species. Although some Asian elephants may have two phalanges in digit I, it is not clearly the predominant pattern, and the proximal sesamoids of manus digit I bear closer anatomical study. High individual variation in these traits and low sample sizes in most studies (1–2 usually) has exacerbated the confusion, and even our sample of 9–10 specimens is too small to draw statistically meaningful generalizations from.

Our use of intact cadaveric specimens rather than defleshed and disarticulated skeletal remains exemplifies the advantages of modern anatomical techniques. Soft tissue data and *in situ* positions are not lost (and are preserved digitally) even once dissections and skeletonization are done. Typical museum specimens have had all of this information scoured clean, reducing the quantity of information that specimens can provide, and potentially leading to anatomical misinterpretations.

3.6 Conclusions

We have provided examples from paleobiological and neontological perspectives on animal limb function (and evolution) to emphasize how the problem of conducting biomechanical analysis is solved from these perspectives, and how anatomical methods ranging from dissection, osteology, and functional morphology, to modern imaging techniques and computer modeling are used similarly or differently in these perspectives. We used an extinct dinosaur (*Velociraptor*) and an extant elephant (*Elephas maximus*) as examples of comparable subjects of interest to paleobiologists and neontologists. Extinct dinosaurs present mainly osteological evidence which can be used to investigate scaling trends of bone shape with size, to analyze simple functional morphology of bony articulations, or to construct complex computer models that add soft tissues to an articulated skeleton in order to more integratively analyze limb mechanics. Dissection of course is impossible; bones are the primary evidence and can themselves be fruitful. Yet the vexing problem that more complex analyses introduce more unknown parameters and hence broader, less specific quantitative results, can be frustrating regardless of the techniques available.

In contrast, such abundant data are accessible in living animals that complex biomechanical analysis becomes a different challenge: what to measure and how, vs. what assumptions must be made about unmeasured parameters? Many parameters may not be measured, simply because of time constraints or often because insufficient animals can be obtained, or invasive experimentation is impossible/undesirable (particularly the case for elephants).

Both perspectives hence share a common theme of balancing (and explicitly engaging with) the known and unknown in order to address research questions. Anatomical analysis forms the foundation of these perspectives as well. However, paleontologists generally proceed from the bones outward to interpret the once-intact whole organism, whereas neontologists typically dissect inwards from the surface of a whole animal, only later to reach the bones. Part of the wonder of modern imaging techniques is that they can reverse the directions of these pathways of inquiry – with computed tomography one can interpret skeletal mechanics in an extant animal without the conventional scalpel, or peer inside irreplaceable fossil bones without harm to them. Our examples show how biomechanical analysis is a field where anatomical inquiry, both classical and modern, is alive and well and offers exciting ways to integrate paleontological and neontological approaches.

Our two case studies also exemplify how new anatomical techniques have synergy with new and old methods in biomechanical analysis (computer simulation of dinosaurs) and phylogenetic studies (comparative anatomy of elephant species). Much as anatomy remains a crucial foundation for phylogenetics (for theropods e.g., Gauthier 1986; Sereno 1999; Xu et al. 2003; for elephants e.g., Shoshani and Tassy 1996; Shoshani 1998; Thomas et al. 2000), it is an often under-appreciated foundation of biomechanical analysis. For example, in order to figure out how a dinosaur stood or moved, we need to calculate how large of a moment each muscle-tendon unit could have generated about its hind limb joints and relate those moments to the moments of gravity, inertia, and ground reaction forces that standing or moving imposed. This is basic Newtonian mechanics, but relies on accurate anatomical data. Our model of muscle moment arms in *Velociraptor* takes one step toward this end, by representing the 3D geometry of the bones and muscle-tendon units. This also

aids in resolving the problem that function often cannot reliably be inferred simply from anatomical form (e.g., Lauder 1995; Koehl 1996) by explicitly quantifying mechanical function, using anatomical geometric data.

The dinosaur model also shows how our elephant modeling will next proceed; surprisingly, dinosaur comparative osteology is much more well described than for elephant limbs, so we needed to fill in this gap first for extant elephants. Now that we have 3D characterizations of limb bone anatomy in Asian elephants, we can export our bone images into musculoskeletal modeling software and combine them with the properties of individual muscle-tendon units (e.g., estimated force-generating capacity) that we are measuring in dissections. Since we know how Asian elephant anatomy differs from African elephants (only very slightly), we can use models to address if and how these anatomical differences affect musculoskeletal mechanics.

Despite these epistemological differences, the fact remains that extant or extinct, dinosaurs and elephants are still organisms. As their anatomy is often same basic components that were just differently ‘tinkered’ (Jacob 1977) together during evolution, the same basic anatomical data are needed regardless of the species being studied, and analysis can proceed in much the same way, even if it must proceed more indirectly and tentatively for extinct taxa. The various disciplines of neontology and paleontology are often separated more by human perspective, history, and bias than by real biological differences. Anatomy is a crucial line of evidence that integrates them all.

Acknowledgments

We thank Silvia Salinas-Blemker for help constructing the *Velociraptor* model, in addition to the expertise of Vern Houston and colleagues at the New York University School of Medicine in laser scanning the bones. Mark Norell is thanked for access to the Mongolian specimens in his care, and trusting JRH to carry them away for scanning. Brian Garner provided expert help in smoothing and reformatting the bone files after scanning. Technical support, advice, and other input along the way from Scott Delp, Peter Loan, and F. Clay Anderson is much appreciated. This work was completed as part of a grant from the National

Science Foundation in 2001. We also thank the staff of Whipsnade Wild Animal Park and other facilities for access to cadaveric elephant specimens, without which our research would be impossible. We thank Richard Prior in the Pathology Department of the Royal Veterinary College for aid during our dissections, and colleagues in the Structure and Motion Laboratory for additional assistance. Funding for the elephant research was provided in 2005 by the BBSRC for New Investigator grant number BB/C516844/1. Additional funding for CT scanning was provided by a University of London Central Research Fund grant in 2005. We appreciate technical support for CT scanning and MIMICS software from Chris Lamb, Renate Weller, Karin Jespers, and Materialize, Inc. Helpful input on this chapter was received from Chris Basu, Cyrille Delmer, Roland Frey, Victoria Herridge, and Gerald Weissengruber.

References

- Alexander R McN (1989) Dynamics of dinosaurs and other extinct giants. Columbia University Press, New York
- Alexander R McN, Ker RF (1990) The architecture of leg muscles. In: Winters JM, Woo SL-Y (eds) Multiple muscle systems. Springer-Verlag, New York, pp 568–577
- Alexander R McN, Jayes AS, Maloiy GMO, Wathuta EM (1981) Allometry of the leg muscles of mammals. *J Zool* 194:539–552
- Alexander R McN, Maloiy GMO, Hunter B, Jayes AS, Nturi J (1979) Mechanical stresses in fast locomotion of buffalo (*Syncerus caffer*) and elephant (*Loxodonta africana*). *J Zool* 189:135–144
- An KN, Takahashi K, Harrigan TP, Chao EY (1984) Determination of muscle orientations and moment arms. *J Biomech Eng* 106:280–283
- Biewener AA (1989) Scaling body support in mammals: limb posture and muscle mechanics. *Science* 245:45–48
- Biewener AA (1990) Biomechanics of mammalian terrestrial locomotion. *Science* 250:1097–1103
- Blair P (1710) Osteographica elephantina. *Phil Trans Roy Soc Lond* 27:51–168
- Carrano MT (1998) Locomotion in non-avian dinosaurs: integrating data from hindlimb kinematics, in vivo strains, and bone morphology. *Paleobiology* 24:450–469
- Carrano MT, Hutchinson JR (2002) Pelvic and hindlimb musculature of *Tyrannosaurus rex* (Dinosauria: Theropoda). *J Morph* 252:207–228
- Charig A (1972) The evolution of the archosaur pelvis and hindlimb: an explanation in functional terms. In: Joysey KA, Kemp TS (eds) Studies in vertebrate evolution. Oliver & Boyd, Edinburgh, UK, pp 121–155
- Coombs WP (1978) Theoretical aspects of cursorial adaptations in dinosaurs. *Q Rev Biol* 53:393–415
- Csuti BA, Sargent EL, Bechert US (eds) (2001) The elephant's foot: care and prevention of foot conditions in

- captive Asian and African elephants. Iowa State Press, Ames
- Delp SL, Hess WE, Hungerford DS, Jones LC (1999) Variation of rotation moment arms with hip flexion. *J Biomech* 32:493–501
- Eales NB (1928) The anatomy of a foetal African Elephant, *Elephas africanus (Loxodonta africana)*. Part II. The body muscles. *Trans Roy Soc Edinburgh* 55:609–642
- Eales NB (1929) The anatomy of a foetal African Elephant, *Elephas africanus (Loxodonta africana)*. Part III. The contents of the thorax and abdomen, and the skeleton. *Trans Roy Soc Edinburgh* 56:203–246
- Farlow JO, Gatesy SM, Holtz TR Jr, Hutchinson JR, Robinson JM (2000) Theropod locomotion. *Am Zool* 40:640–663
- Gambaryan PP (1974) How mammals run. John Wiley & Sons, New York
- Gatesy SM (1990) Caudofemoral musculature and the evolution of theropod locomotion. *Paleobiol* 16:170–186
- Gauthier JA (1986) Saurischian monophyly and the origin of birds. In: Padian K(ed.) The origin of birds and the evolution of flight. *Mem Calif Acad Sci* 8:1–55
- Hutchinson JR (2001a) The evolution of pelvic osteology and soft tissues on the line to extant birds (Neornithes). *Zool J Linn Soc* 131:123–168
- Hutchinson JR (2001b) The evolution of femoral osteology and soft tissues on the line to extant birds (Neornithes). *Zool J Linn Soc* 131:169–197
- Hutchinson JR (2002) The evolution of hindlimb tendons and muscles on the line to crown-group birds. *Comp Biochem Physiol A* 133:1051–1086
- Hutchinson JR (2004a) Biomechanical modeling and sensitivity analysis of bipedal running ability. I. Extant taxa. *J Morph* 262:421–440
- Hutchinson JR (2004b) Biomechanical modeling and sensitivity analysis of bipedal running ability. II. Extinct taxa. *J Morph* 262:441–461
- Hutchinson JR, Garcia M (2002) *Tyrannosaurus* was not a fast runner. *Nature* 415:1018–1021
- Hutchinson JR, Gatesy SM (2000) Adductors, abductors, and the evolution of archosaur locomotion. *Paleobiology* 26:734–751
- Hutchinson JR, Famini D, Lair R, Kram R (2003) Biomechanics: are fast-moving elephants really running? *Nature* 422:493–494
- Hutchinson JR, Anderson FC, Blemker S, Delp SL (2005) Analysis of hindlimb muscle moment arms in *Tyrannosaurus rex* using a three-dimensional musculoskeletal computer model. *Paleobiology* 31:676–701
- Hutchinson JR, Schwerda D, Famini D, Dale RHI, Fischer M, Kram R (2006) The locomotor kinematics of African and Asian elephants: changes with speed and size. *J Exp Biol* 209:3812–3827
- Jacob F (1977) Evolution and tinkering. *Science* 196:1161–1196
- Koehl MAR (1996) When does morphology matter? *Ann Rev Ecol Syst* 27:501–542
- Lauder GV (1995) On the inference of function from structure. In: Thomason JJ (ed.) *Functional morphology in vertebrate paleontology*. Cambridge University Press, Cambridge, pp 1–18
- Mariappa D (1986) *Anatomy and histology of the Indian elephant*. Indira Publishing House, Oak Park, MI
- Neuville H (1935) Sur quelques caractères anatomiques du pied des éléphants. *Arch Mus Nat d'Hist Natur Paris* 6e Série 13:111–183
- Paul GS (1998) Limb design, function and running performance in ostrich-mimics and tyrannosaurs. *Gaia* 15:257–270
- Payne RC, Veenman P, Wilson AM (2004) The role of the extrinsic thoracic limb muscles in equine locomotion. *J Anat* 206:193–204
- Payne RC, Hutchinson JR, Robilliard JJ, Smith NC, Wilson AM (2005) Functional specialization of pelvic limb anatomy in horses (*Equus caballus*). *J Anat* 206:557–574
- Perle A (1985) Comparative myology of the pelvic-femoral region in the bipedal dinosaurs. *Paleontol J* 19:105–109
- Ramsay EC, Henry RW (2001) Anatomy of the elephant foot. In: Csuti BA, Sargent EL, Bechert US (eds) (2001) *The Elephant's Foot: Care and Prevention of Foot Conditions in Captive Asian and African Elephants*. Ames: Iowa State Press, pp 9–12.
- Romer AS (1927) The pelvic musculature of ornithischian dinosaurs. *Acta Zoologica* 8:225–275
- Roth VL (1984) How elephants grow: heterochrony and the calibration of developmental stages in some living and fossil species. *J Vert Paleont* 4:126–145
- Sereno PC (1999) The evolution of dinosaurs. *Science* 284:2137–2147
- Shoshani J (1998) Understanding proboscidean evolution: a formidable task. *Trends Ecol Evol* 13:480–487
- Shoshani J, Tassy P (eds) (1996) *The Proboscidea: evolution and palaeoecology of elephants and their relatives*. Oxford University Press, Oxford
- Sikes SK (1971) *The natural history of the African elephant*. Weidenfeld and Nicolson, London
- Smuts MMS, Bezuidenhout AJ (1993) Osteology of the thoracic limb of the African elephant (*Loxodonta africana*). *Ontarstepoort J Vet Res* 60:1–14
- Smuts MMS, Bezuidenhout AJ (1994) Osteology of the pelvic limb of the African elephant (*Loxodonta africana*). *Ontarstepoort J Vet Res* 61:51–66
- Thomas MG, Hagelberg E, Jones HB, Yang Z, Lister AM (2000) Molecular and morphological evidence on the phylogeny of the Elephantidae. *Proc Roy Soc Lond B* 267:2493–2500
- Walker AD (1977) Evolution of the pelvis in birds and dinosaurs. In: Andrews SM, Miles RS, Walker AD (eds) *Problems in vertebrate evolution*, Linn Soc Symp Ser 4. Academic Press, London, pp 319–358
- Weissengruber GE, Egger GF, Hutchinson JR, Groenewald HB, Elsässer L, Famini D, Forstenpointner G (2006) The structure of the cushions in the feet of African Elephants (*Loxodonta africana*). *J Anat* 209:781–792
- Witmer LM (1995) The extant phylogenetic bracket and the importance of reconstructing soft tissues in fossils. In: Thomason JJ (ed.) *Functional morphology in vertebrate paleontology*. Cambridge University Press, Cambridge, pp 19–33
- Xu X, Zhou Z, Wang X, Kuang X, Zhang F, Du X (2003) Four-winged dinosaurs from China. *Nature* 6921:335–340
- Zajac FE (1989) Muscle and tendon: properties, models, scaling, and application to biomechanics and motor control. *Crit Rev Biomed Eng* 17:359–411